Assessment of Hepatic Focal Lesions Using Liver Imaging Reporting and Data System (LI- RADS)

Haidy Hany Eissa*, Marwa Mohamed Romeih, Medhat Mohamed Reffat*, Hamada Mohamed Khater***

*Radiology Department, faculty of medicine, Benha University, **Radiology Department, faculty of medicine, Helwan University.

Corresponding author: Haidy Hany Eissa, Radiology Department, faculty of medicine, Benha University.

hhm.eissa@gmail.com

ABSTRACT

Background: The Liver Imaging and Reporting Data System (LI-RADS) is a comprehensive system for standardizing the terminology, technique, interpretation, reporting, and data collection of liver imaging. The aim of this work was to evaluate the diagnostic performance of LI-RADS version 2017 major features, ancillary features, and categories on Triphasic CT, U/S and MRI for the diagnosis of HCC. **Methods:** This prospective study was carried out on 70 patients aged over 18 years old, both sexes, with clinical criteria high risks for HCC (Liver cirrhosis, chronic viral hepatitis infection from hepatitis B virus even in absence of cirrhosis, alcoholic steatohepatitis, and non-alcoholic steatohepatitis, or current or previously diagnosed HCC) who were suspected either clinically or by previous cross sectional imaging study (US, CT and MRI) to have a hepatic lesion. Patient further subdivided into two groups: HCC group and non-HCC group. All patients were subjected to triphasic CT, dynamic MRI liver was done on 10 patients. **Results:** Pre contrast, late arterial, venous washout, LIRAD were significantly higher in HCC group than non-HCC group (P value<0.05). There were significant differences regarding border (Infiltrative, ill-defined, ill-defined exophyte, well defined, and exophytic), and LIRAD types between both groups (P= 0.002, <0.001 respectively). LIRAD can significantly predict diagnosis of HCC (P value<0.001 and AUC=0.813) with 100% sensitivity, 62.5% specificity, 90.3% +PV 100% -PV and 91.86% accuracy.

Introduction

Hepatocellular carcinoma (HCC) ranks as the second most prevalent primary liver malignancy globally in terms of cancer-related mortality [1]. Well-established risk factors for HCC include chronic viral hepatitis infection caused by hepatitis B virus (HBV), cirrhosis, alcoholic steatohepatitis, and non-alcoholic steatohepatitis (NASH) [2].

The prognosis for patients diagnosed with symptomatic HCC is bleak, with a median 5-year survival rate of less than 10%. Nevertheless, this figure significantly improves to 58% in patients who undergo curative therapy consisting of liver resection or liver transplantation [3].

Significant progress has been made in recent years regarding the multimodal treatment of HCC, which has resulted in a more effective prognosis for HCC patients. As a result, for the purpose of treatment planning, systematic screening, early detection of liver nodules, precise diagnosis of HCC, and tumor staging have grown in significance [4].

Imaging plays a crucial role in the therapy of patients who have been diagnosed with liver cancer, whether it is confirmed or suspected. With the high specificity and confidence of multiphasic computed tomography (CT) or magnetic resonance imaging (MRI), HCC can be diagnosed non-invasively. This eliminates the need for percutaneous biopsy, which carries risks such as tumor seeding and bleeding, and enables the majority of patients to bypass the procedure [5].

Therefore, consistent reporting and precise image interpretation by radiologists are crucial for the diagnosis of HCC. An address for imaging and reporting systems is required in order to furnish specific criteria for HCC diagnosis, a diagnostic algorithm, and reporting obligations. Multiple societies have advocated for the implementation of structured radiology reporting and diagnostic systems, which have demonstrated the ability to enhance the overall positive predictive value (PPV) in the diagnosis of malignancy [5].

The Liver Imaging and Reporting Data System (LIRADS) is a comprehensive framework that has been specifically developed to establish standardized practices for imaging the liver. Its functionalities encompass technique, interpretation, terminology, data collection and reporting. Developed by a multidisciplinary group comprising diagnostic and interventional radiologists, hepatologists, hepatobiliary surgeons, and hepatopathologists, it has the endorsement of the American College of Radiology (ACR). The principal aims of LIRADS are to reduce inaccuracies and fluctuations in interpretation [6].

This trial's purpose was to assess the diagnostic performance of major features, ancillary features, and categories of LI-RADS version 2017 on Triphasic CT, U/S, and MRI in the detection of HCC.

Patients and Methods

A prospective study was carried out on a cohort of 70 patients, both male and female, who met the following clinical and cross-sectional imaging criteria: high risk for HCC (liver cirrhosis, chronic viral hepatitis infection from HBV even in the absence of cirrhosis, alcoholic steatohepatitis, NASH, or current or previously diagnosed HCC); suspicion of a hepatic lesion (US, CT, and MRI).

Written informed consent was obtained from the patient or their legal guardians. The trial was conducted with the ethical committee of the Tanta Cancer Center's (TCC) approval from **January 2022 to January 2023.**

Patients who failed to meet the inclusion criteria were those who were below the age of 18, had a history of iodine contrast allergy, or had cirrhosis caused by congenital hepatic fibrosis or vascular disorders (e.g., Budd-Chiari syndrome).

Patients are additionally divided into two cohorts: those with HCC and those without.

Triphasic CT was performed on all patients, while dynamic MRI of the liver was performed on ten patients only, whose CT triphasic study was not conclusive to diagnose and needed dynamic MRI study.

CT examination protocol design

Triphasic CT examinations were conducted utilizing a GE light speed VCT 64 multislice CT scanner.

Each patient underwent a craniocaudal scan while in the supine position.

In the initial stage, conventional spiral mode non-enhanced spiral scanning was executed with a tube voltage of 120 kVp (180 milliampere seconds, 0.8 pitch, 0.5 s/rotation, DFOV 42 cm2, matrix 512 3 512, and 32 3 1.2-mm collimation).

As a result, the patients were administered non-ionic contrast material (Ultravist 370; Bayer Schering Pharma, Berlin,

Germany) through peripheral venous access at a flow rate of 3.0 mL/sec. Injecting 90–120 mL (1.5 mL per kg of body weight) into the subject was accomplished with a CT-compatible power injector.

During the delayed phase, portal-venous phase, and late hepatic arterial phase, scans were obtained. The scanning delay for late hepatic arterial phase imaging was measured utilizing G.E. Healthcare's automated scan triggering software. Upon reaching the trigger attenuation threshold of 100 HU at the level of the supra-celiac abdominal aorta, the arterial phase scan was automatically initiated 10–15 seconds later. After thirty seconds had passed since the arterial phase scan, the hepatic portal venous phase scan was initiated. 2-7 minutes following the end of arterial phase scanning, a delayed phase was executed.

MRI examination

A 1.5 T scanner (Achieva, Philips Medical Systems, Best, Netherlands, Release 2.6, Level 3) was utilized for the procedure. Pre-contrast imaging was conducted using MRI sequences and an EP MR injection system subsequent to the bolus injection of 0.1mmol/kg body weight of Gd-DTPA via automatic injector.

Dynamic imaging utilizing a T1-weighted gradient echo sequence with 3D fat suppression (THRIVE, or T1 high resolution isotropic volume examination). One pre-contrast series was succeeded by four post-contrast series, each encompassing the early arterial, late arterial, and portal phases, with intervals of 19 to 21 seconds (17 seconds for image acquisition while holding the breath and 2-4 seconds for re-breathing). Subsequently, a 5-minute delayed phase imaging sequence was executed. Patients were imaged at the end of expiration to minimize the potential of image misregistration.

The 1.5 Tesla machines utilized the following acquisition parameters: TR 10 msec, TE 4.6 msec, flip angle 15°, matrix size 172x163, field of view 300–350 mm, and slice thickness 7 mm.

The CT and MRI images proceeded on workstation:

The hepatic imaging specialist had two readers assess the CT or MRI examination while remaining oblivious to the pathology outcome. Using the LIRADS system (2017 v), the reader assessed each hepatic focal lesion in an independent manner.

All images were devoid of the acquisition date and participant identification information. All clinical information was withheld from the radiologist. In order to assess "threshold growth" as defined by LIRADS, the readers were furnished with prior cross-sectional imaging studies (CT or MRI), if accessible.

LIRADS was employed to assess six imaging characteristics for each hepatic focal lesion: tumor diameter, arterial phase hyper-enhancement, washout appearance, capsule, tumor embolus within a vein lumen, and, if feasible, tumor growth rate.

The reader then assigned a final LIRADS score among one and five using the following procedure: LR-1 and LR-2 were assigned to definitely benign and probably benign lesions, respectively, before LR-3, LR-4, and LR-5 were classified in accordance with LIRADS. The assignment of LR-3, LR-4, and LR-5 was determined by selecting the corresponding columns and rows in the LIRADS table. The diameter and enhancement pattern (arterial phase hypo-enhancement or iso-enhancement versus hyper-enhancement) were utilized to select the column. The row was chosen based on the quantity of major characteristics that were present, including washout appearance, capsule, and threshold growth. Subsequently, the suitable category was identified by intersecting the selected column and row.

It is noteworthy that in the LIRADS version 2017, observations corresponding to

specific macrovascular venous invasion are designated with the abbreviation LR-TIV. This abbreviation is maintained even in the absence of imaging identification of a parenchymal mass. The reader was not granted access to any subsequent screening. In order to assess "threshold growth" as defined by LIRADS, the readers were furnished with prior cross-sectional imaging studies (CT or MRI), if accessible. In addition, if a patient underwent multiple observations, a distinct LIRADS score was assigned to each individual lesion.

We divided the lesions into two distinct categories: those with HCC and those without. The malignant lesions were identified through histologic examination subsequent to biopsy or surgical intervention. These lesions were subsequently classified as HCC lesions; benign lesions were identified through follow-up with cross-sectional imaging (e.g., US, CT, or MRI) or histopathology, if available. The non-HCC group comprised patients who had pathologically confirmed benign lesions, as well as those who lacked pathological confirmation and did not meet the integrative-evaluation criteria (IEC) for HCC.

The integrative-evaluation criteria (IEC) for HCC:

In addition to possessing a medical history that includes chronic viral hepatitis and/or cirrhosis, the candidate must demonstrate the following: elevated levels of serum a-fetoprotein (>11 ng/mL), consistent detection of HCC-related findings on CT/MR images or digital subtraction angiography during TACE treatment, and a prepondinance of iodized oil uptake at one or more follow-up CT examinations performed every four weeks after TACE.

Statistical analysis

SPSS v26 was utilized for the statistical analysis (IBM Inc., Armonk, NY, USA). The quantitative variables were expressed as the mean and standard deviation (SD), and an unpaired Student's t-test was utilized to compare them among the two groups. The percentage (%) and frequency values of qualitative variables were utilized in the analysis, with the appropriate tests being the Chi-square test or Fisher's exact test. Using Receiver Operating Characteristic curve (ROC-curve) analysis, the overall diagnostic performance of each test was evaluated; a curve extending from the lower left corner to the upper left corner and then to the upper right corner indicates a perfect test. The overall performance of the test is assessed by the area under the curve (AUC), with an acceptable performance indicated by an AUC greater than 50% and an optimal performance indicated by an area around 100%. Statistical significance was defined as a two-tailed P value below 0.05.

Results

This study was conducted at radio-diagnosis department of Tanta Cancer Center (TCC). Of the 70 included patients, 73 hepatic focal lesions were determined by CT imaging. This included 55 HCC lesions, and 18 non-HCC lesions (2 atypical hemangiomas, 1 steatosis, 1 simple cyst, 2 dysplastic nodules, 7 typical haemangiomas, 1 focal nodular hyperplasia, 1 cholangiocarcinoma and 3 metastatic lesions).

The data in **Error! Not a valid bookmark self-reference.** indicates that the mean age was 60.4 ± 9.29 years. 18 (25.71%) were females and 52 (74.29%) were male. Cirrhosis was the cause of liver parenchyma in 65 (92.86%) of the patients, fatty in 3 (4.29%), and normal in 2 (2.86%). Lesions were present in 25 (35.71%) patients, one in 38 (54.29%) patients, and two in seven (10%) patients. A total of 23 patients (32.86%) had portal vein tumors, 25 patients (35.71%) had LN metastases, 14 patients (20%) had bony metastatic lesions (lower dorsal and lumbar vertebrae), and ascites was mild in 10 patients (14.29%), moderate in 1 patient (1.43%), and marked in 2 patients (2.86%). A total of 70 triphasic CT studies (100

percent) and 10 dynamic MRI studies (14.3 percent) were analyzed.

Table 1: Demographic data, tumor in vein, LN, metastasis, ascites and examination of the studied patients (n = 70):

		Patients (n = 70)
Age (years)		60.4 ± 9.29
Sex	**Male**	52 (74.29%)
	Female	18 (25.71%)
Liver parenchyma	**Cirrhosis**	65 (92.86%)
	Fatty	3 (4.29%)
	Normal	2 (2.86%)
Number of lesions	**1**	38 (54.29%)
	2	7 (10%)
	Multiple	25 (35.71%)
Tumor in vein (PV)		23 (32.86%)
LN		25 (35.71%)
Metastasis		14 (20%)
Ascites	**Mild**	10 (14.29%)
	Moderate	1 (1.43%)
	Marked	2 (2.86%)
	No	57 (81.43%)
CT		70 (100%)
MRI		10 (14.3%)

Data are presented as mean ± SD or frequency (%). PV: predictive value, LN: lymph node, CT: computed tomography, MRI: magnetic resonance imaging.

The HCC group exhibited significantly higher values of pre-contrast (hypo, hyper, and iso dense), late arterial (no enhancement, hypo or iso, and hyper enhancement), venous washout, and LIRAD (positive and negative) in comparison to the non-HCC group (P value<0.05). In both groups, border characteristics (ill-defined, exophyte, well-defined, and exophytic) and LIRAD types (LR1, LR2, LR3, LR4, LR5, and LRm) differed significantly (P=0.002 and <0.001, respectively). The tumor site (bilobed, right, left) and capsule (capsule, and absence of capsule) did not differ significantly among the HCC and non-HCC groups. The HCC group exhibited lesions with a mean size of 7.93 ± 4.53 cm. **Table 2.**

The current investigation revealed that cirrhosis characterized the liver parenchyma of 65 (92.86%) of the patients, fatty parenchyma of 3 (4.29%), and normal parenchyma of 2 (2.86%). Lesions were present in 25 (35.71%) patients, one in 38 (54.29%) patients, and two in seven (10%) patients. The dimensions of the lesions varied from 0.6 to 18 cm. **(Figure 2,3,4)**

LIRAD can predict HCC diagnosis with a significant degree of accuracy (91.86%), 62.5% specificity, 90.3% +PV, and 100% -PV (P value<0.001 and AUC=0.813). **Figure 1**

Figure 1

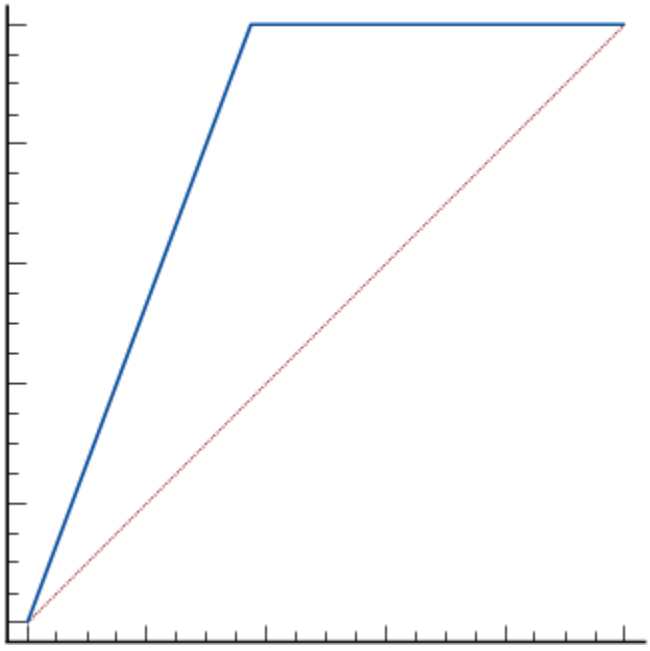

Figure 1: Roc curve of LIRAD in prediction of diagnosis of HCC of the studied patients.

Table 2: Summary of major features using LIRADS, LIRAD significance, and types in HCC and Non-HCC groups:

		HCC group	Non-HCC group	P value
Site of tumor	**Right**	**22 (38.6%)**	**6 (35.29%)**	**0.353**
	Left	**17 (29.82%)**	**8 (47.06%)**	
	Bilobed	**18 (31.58%)**	**3 (17.65%)**	
Pre contrast	**Hypo dense**	**57 (100%)**	**13 (76.47%)**	**0.001***
	Hyper dense	**0 (0%)**	**3 (17.65%)**	
	Iso dense	**0 (0%)**	**1 (5.88%)**	
Late arterial enhancement	**No enhancement**	**0 (0%)**	**5 (29.41%)**	**<0.001***
	Hypo or iso enhancement	**22 (37.93%)**	**3 (17.65%)**	
	hyper enhancement	**35 (60.34%)**	**9 (52.94%)**	
Venous washout		**44 (77.19%)**	**5 (29.41%)**	**0.001***
Capsule	**Capsule**	**18 (31.58%)**	**3 (17.65%)**	**0.364**
	No capsule	**39 (68.42%)**	**14 (82.35%)**	
Border	**Infiltrative**	**1 (1.75%)**	**0 (0%)**	**0.002***
	Ill defined	**44 (77.19%)**	**6 (35.29%)**	
	Ill defined, exophyte	**1 (1.75%)**	**0 (0%)**	
	Well defined	**5 (8.77%)**	**9 (52.94%)**	
	Exophytic	**6 (10.53%)**	**2 (11.76%)**	
Size of lesion (cm)		**7.93 ± 4.53**	**--**	**--**
Threshold growth		**1(1.75 %)**	**2(11.1 %)**	**0.592**
LIRAD	**Positive**	**57 (100%)**	**5 (29.4%)**	**<0.001***
	Negative	**0 (0%)**	**12 (70.6%)**	
LIRAD Types	**LR1**	**0 (0%)**	**3 (37.5%)**	**<0.001***
	LR2	**0 (0%)**	**4 (50%)**	
	LR3	**5 (8.77%)**	**6 (75%)**	
	LR4	**21 (36.84%)**	**1 (12.5%)**	
	LR5	**31 (54.39%)**	**2 (25%)**	
	LRm	**0 (0%)**	**1 (12.5%)**	

Data are presented as frequency (%). LIRAD: Liver Imaging Reporting and Data System. *: significant as P value < 0.05

Discussion

HCC is among the most prevalent types of tumors worldwide. The primary risk factor for HCC development in chronic viral infections patients (specifically hepatitis B and C) and excessive alcohol consumption is liver cirrhosis. HCC is distinguished by distinct tumor characteristics on multislice contrast-enhanced CT or MRI, which enable precise HCC diagnosis without the need for an invasive confirmation procedure [7].

Aly et al. [7] documented that the majority of patients (67.1%) exhibited malignant lesions, with HCC being the most prevalent (45.9%), followed by cholangiocarcinoma (8.2%), and finally hepatic deposits (7.1%). Out of the 39

HCC cases examined, 35 (89.7%) were accurately classified as HCC (LR-5), while 4 (10.3%) tumors were likely HCC (LR-4). All of them were not erroneously identified as benign (LIRAD1) or undifferentiated (LR-M).In the present study, it was found that tumor in portal vein was present in 23 (32.86%) patients, LN metastasis was present in 25 (35.71%) patients, bony metastatic lesions was present in 14 (20%) patients (lower dorsal and lumbar vertebrae) and ascites was mild in 10 (14.29%) patients, moderate in 1 (1.43%) patient, marked in 2 (2.86%) patients.

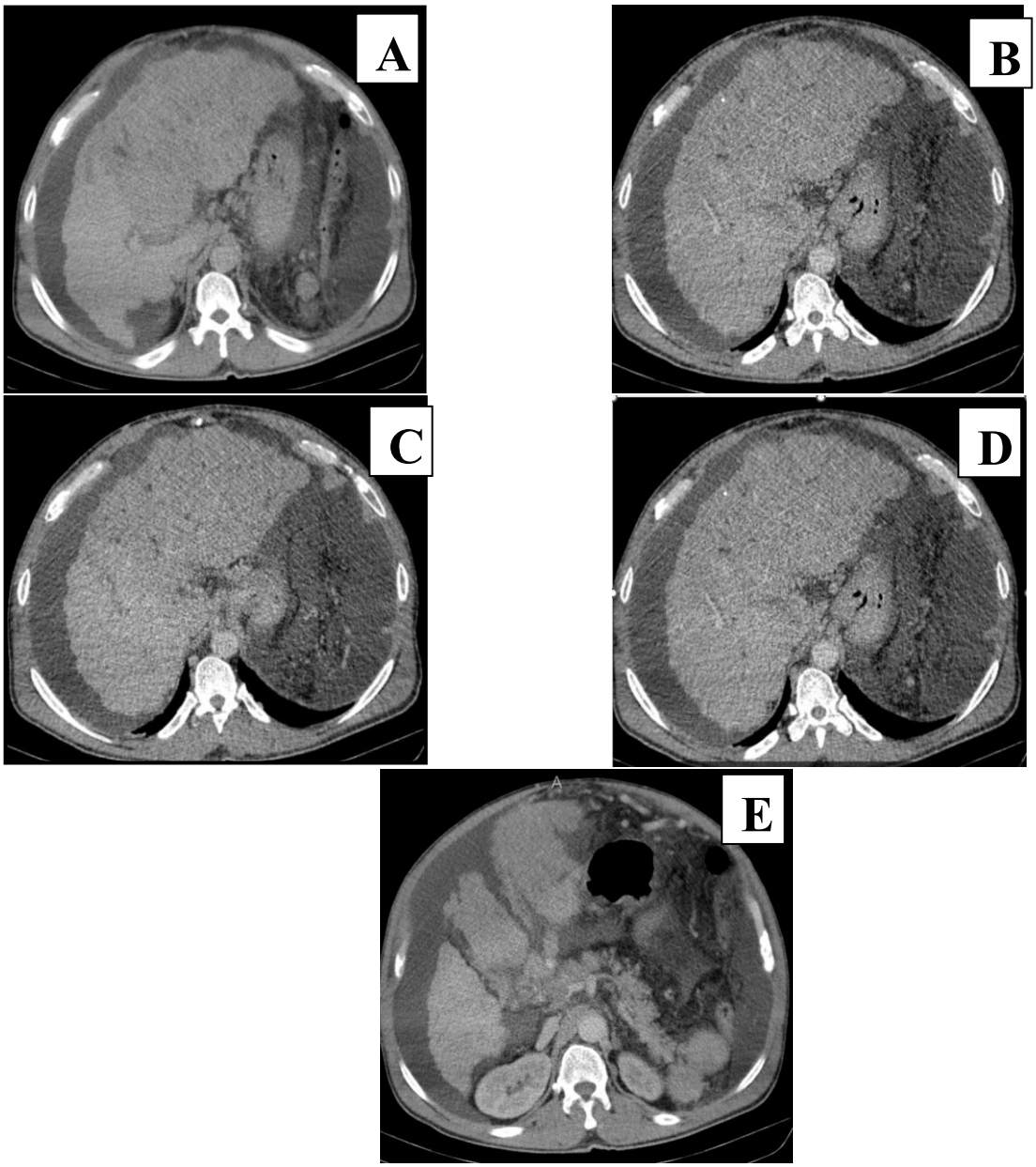

Figure 2: Triphasic CT study of a 56-year-old male patient with chronic hepatitis and HCC.

Aly et al. [7] stated that about 23 patients were diagnosed (27.1%): 14 regenerative hepatic nodules (16.5%), 9 hepatic hemangiomas (10.6%) and finally, focal nodular hyperplasia-

FNH, confluent hepatic fibrosis and biliary cyst adenoma with each representing one patient (1.2 %)

74 hepatic focal lesions were identified by CT imaging in the present study, which involved 70 patients. This included 57 HCC lesions, and17 non-HCC lesions **(Figures 5,6& 7)** (2 atypical hemangiomas, 1 steatosis, 1 simple cyst, 2 dysplastic nodules, 7 typical hemangiomas, 1 focal nodular hyperplasia,1cholangiocarcinoma and 2 metastatic lesions).

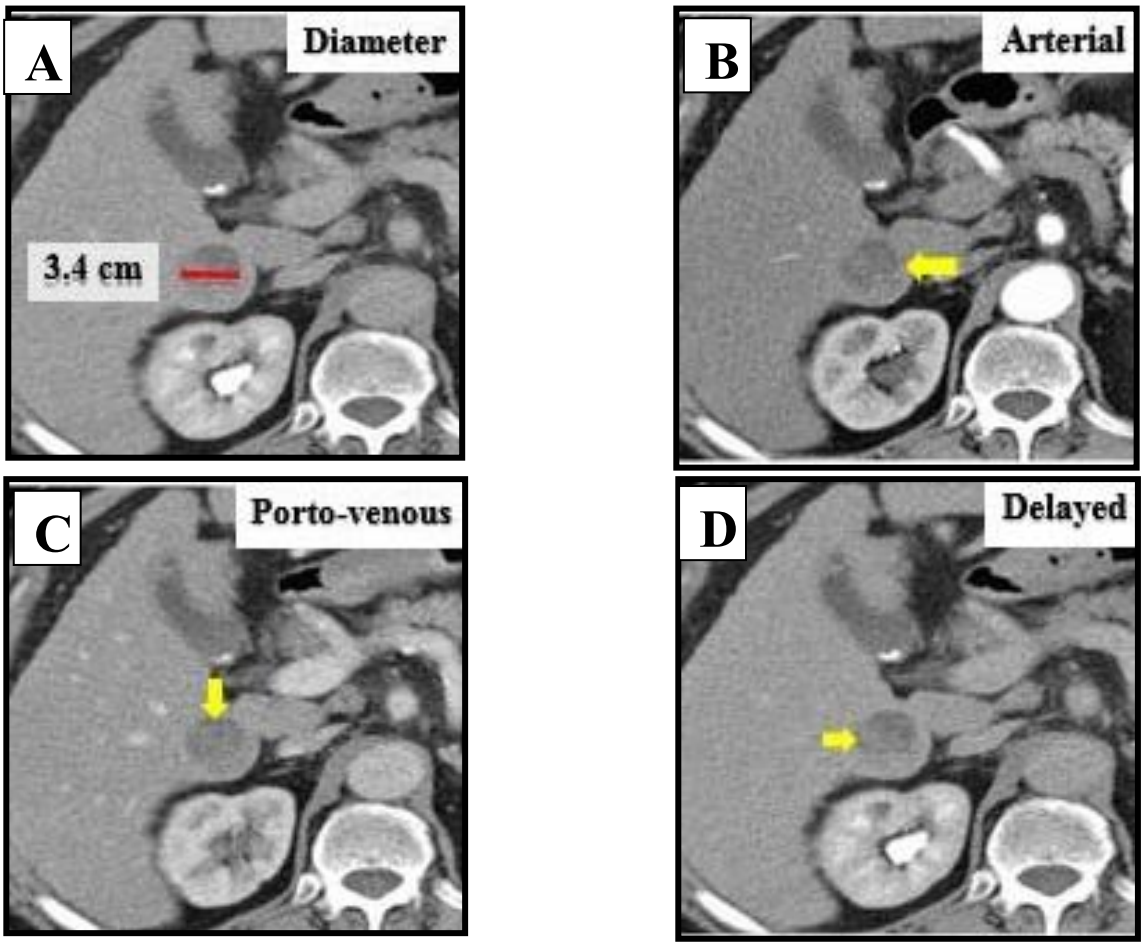

Figure 3: Triphasic CT study of a 63 years old male patient with liver cirrhosis and hepatic focal lesion confirmed by biopsy to be focal steatosis

Aly et al. [7] indicated that hemangioma was the most common among LIRAD1 group (60%), regeneration nodule among LI-RAD 2 group (88.9%), dysplastic nodule among both LI-RAD3 (50%) and LI-RAD 4 groups (55.6). HCC among LI-RAD5 group (100%). Finally, cholangiocarcinoma among LRM group (53.8 %).

Late arterial and venous washout were significantly greater in the HCC group than in the non-HCC group, according to the present trail (P value = 0.05). The HCC group exhibited lesions with a mean size of 7.93 ± 4.53 cm. The LIRAD and LIRAD types were significantly greater in the HCC group compared to the non-HCC group (P <0.001). LIRAD is a highly accurate predictor of HCC diagnosis (AUC=0.813, P value= 0.001, 62.5% specificity, 90.3% +PV 100% -PV), and

91.86% sensitivity (P value=0.001). In diagnosing HCC, LIRADS achieved exceptional levels of accuracy (91.86%), sensitivity (100%) and specificity (62.5%).

An et al. [8] reported that patients who had been diagnosed with hepatocellular carcinoma exhibited significantly higher occurrence rates of key imaging characteristics, such as capsule appearance, washout appearance, and arterial phase hyperenhancement. A minimum of one reviewer deemed the assessment of arterial-phase MR images to be suboptimal in seven instances due to severe motion artifacts or premature acquisition. On MRI, diffuse arterial hyperenhancement and washout appearance were more frequently detected in the transitional or portal phases of HCC lesions compared to CT (88.2% vs. 82.5% [p = 0.015] and 90.4% vs. 77.2% [p = 0.005], respectively). However, when washout appearance was measured solely in the portal phase, the frequency of washout appearance on MRI decreased from that on CT (71.1% vs. 77.2% [p = 0.034]).

On the contrary, Kim et al. [9] confirmed that the most important findings related to HCC, in lesions less than 2 cm, were arterial phase hyperenhancement.

In this concern, De Gaetano et al. [10]enhancing "capsule" showed a high specificity of 88.5% for HCC. This feature was significantly correlated to the histological classification of nodules and was most frequently observed in HCCs.

Corona enhancement is seen as an enhancement in the peritumoral parenchyma and considered as a feature of hypervascular HCC. It begins a few seconds after lesion enhancement, so that with apparent larger tumor size, tumor and corona enhancement may overlap. Its presence aids to distinguish highly vascular HCCs from pseudo-lesions; however, it is not a marker of HCC [11].

The superior ability of gadoxetate-enhanced MRI to exhibit imaging characteristics that favor malignancies may account for its higher sensitivity in differentiating hepatic lesions. Consistent with a recently published study, gadoxetate-enhanced MRI revealed a higher prevalence of arterial hyperenhancement and washout appearance in HCCs compared to CT [12].

On the contrary, previous trails have indicated that the accuracy of gadoxetate-enhanced MRI and CT in discerning HCCs from other types of malignancies was similar. Specifically, both techniques exhibited shortcomings in precisely differentiating HCC from other malignancies, especially combined HCC-CCA[13-16]. Additionally, comparable to a prior report [13]

An et al. (2019) discovered that the inclusion of auxiliary features modified the LI-RADS categories in 12% (111/924) of the cases examined [8]. This finding is similar to two more recent studies (15.3% and 18.1%)[17, 18].

The inclusion of auxiliary features did not yield a statistically significant improvement in the overall LI-RADS categorization, according to one study. Nevertheless, ten benign lesions that were originally classified as LR-5/5V were accurately downgraded. Two recent extracellular contrast media studies yielded contradictory findings regarding the diagnostic performance impact of upgrading LR-3 to LR-4 on the basis of ancillary features [17, 19].

It was recommended that routine surveillance be maintained without further testing for the benign LR2 category, which contradicts the majority of scientific guidelines for the diagnosis of HCC.

A retrospective study conducted by Choi et al. [20] revealed that a mere 6% of LR3 lesions were classified as probable or definitive HCCs. As a result, they recommended routine monitoring of the LR3 lesions

The findings of that research were exclusively derived from nodules identified via

ultrasound screening, thereby augmenting the probability prior to the examination. In addition, hepatitis B was present in more than 98% of our patients compared to 72% of the patients in the clinical trial. Gross specimens of cirrhosis obtained from patients with diverse hepatitis B or C backgrounds displayed discernible morphological characteristics subsequent to surgical resection.

LI-RADS OM is defined as the presence of malignancies other than HCC that have a high probability of being detected. Three (or 25%) of the twelve cases of LRM included in our trail were HCC. Due to the fact that distinct types of malignant tumors require distinct clinical treatments and have distinct prognoses, an accurate preoperative diagnosis is critical. The existing LI-RADS diagnostic system, however, still necessitates enhancements.

Darnell's research endeavors were guided by the AASLD and EASL-EORTC recommendations, which stipulated the strict monitoring of nodules with a diameter not exceeding 10 mm. HCC comprised two of the category 4 lesions (<10 mm) and three of the seven lesions (>10 mm) included in this study, as reported by Darnell's cohort data. This finding is in opposition to their suggestion concerning LI-RADS category 2 lesions, which possess a 5–10% likelihood of progressing to HCC and thus should not be disregarded. Five lesions with a diameter of less than 10 mm were initially classified as LR4 but were later determined to be HCCs in our cohort [21].

Consequently, we suggest the establishment of a separate work-up schedule specifically designed for imaging-detected nodules classified as LI-RADS and measuring less than 10 mm. Active diagnostic testing for LR4 lesions is strongly recommended, considering that the aim of preventive medicine is to detect and manage HCC while it is still in its early stages. Additional research is necessary to validate the most effective follow-up strategy for the lower categories (LR2 or 3).

One of the limitations is: The research design was a single-centre retrospective study, which may have introduced some selection bias in the patients. Additionally, the diagnostic performance of CECT was investigated, but we did not assess ancillary features of LIRADS or whether their application could have reduced the number of "indeterminate" LR-3 observations and enabled more frequent benign or malignant categorization. Therefore, prospective studies with paired image data and larger sample sizes are required, as well as single-center research with a small sample size and some in-patient selection bias.

Conclusions

The LI-RADS provides diagnostic guidance that is specifically designed to distinguish HCC from other focal lesions of the liver in high-risk patients, with the ultimate goal of achieving optimal management.

Financial support and sponsorship: Nil

Conflict of Interest: Nil

References

1. Torre LA, Bray F, Siegel RL, Ferlay J, Lortet-Tieulent J, Jemal A. Global cancer statistics, 2012. CA Cancer J Clin. 2015;65:87-108.

2. Nishikawa H, Osaki Y. Liver Cirrhosis: Evaluation, Nutritional Status, and Prognosis. Mediators Inflamm. 2015;2015:872152.

3. Dhir M, Lyden ER, Smith LM, Are C. Comparison of outcomes of transplantation and resection in patients with early hepatocellular carcinoma: a meta-analysis. HPB (Oxford). 2012;14:635-45.

4. Schima W, Heiken J. LI-RADS v2017 for liver nodules: how we read and report. Cancer Imag. 2018;18:14.

5. Song DS, Bae SH. Changes of guidelines diagnosing hepatocellular carcinoma during the last ten-year period. Clin Mol Hepatol. 2012;18:258-67.

6. Elsayes KM, Kielar AZ, Elmohr MM, Chernyak V, Masch WR, Furlan A, et al. White paper of the Society of Abdominal Radiology hepatocellular carcinoma diagnosis disease-focused panel on LI-RADS v2018 for CT and MRI. Abdom Radiol (NY). 2018;43:2625-42.

7. Aly RA, Abokoura S. Employing li-rads on dynamic mri scans for distinguishing hepatocellular carcinoma from other hepatic focal lesions in high risk patients. Ain Shams Med J. 2023;74:635-53.

8. An C, Lee CH, Byun JH, Lee MH, Jeong WK, Choi SH, et al. Intraindividual comparison between gadoxetate-enhanced magnetic resonance imaging and dynamic computed tomography for characterizing focal hepatic lesions: a multicenter, multireader study. Korean J Radiol. 2019;20:1616-26.

9. Kim TK, Lee KH, Jang HJ, Haider MA, Jacks LM, Menezes RJ, et al. Analysis of gadobenate dimeglumine–enhanced MR findings for characterizing small (1–2-cm) hepatic nodules in patients at high risk for hepatocellular carcinoma. J Radiol 2011;259:730-8.

10. De Gaetano AM, Catalano M, Pompili M, Marini M, Rodríguez Carnero P, Gullì C, et al. Critical analysis of major and ancillary features of LI-RADS v2018 in the differentiation of small (≤ 2 cm) hepatocellular carcinoma from dysplastic nodules with gadobenate dimeglumine-enhanced magnetic resonance imaging. Eur Rev Med Pharmacol Sci. 2019;23:34-44.

11. Choi J-Y, Lee J-M, Sirlin CB. CT and MR imaging diagnosis and staging of hepatocellular carcinoma: part II. Extracellular agents, hepatobiliary agents, and ancillary imaging features. J Radiol 2014;273:30-50.

12. Kim YN, Song JS, Moon WS, Hwang HP, Kim YK. Intra-individual comparison of hepatocellular carcinoma imaging features on contrast-enhanced computed tomography, gadopentetate dimeglumine-enhanced MRI, and gadoxetic acid-enhanced MRI. Acta radiol. 2018;59:639-48.

13. Fraum TJ, Tsai R, Rohe E, Ludwig DR, Salter A, Nalbantoglu I, et al. Differentiation of hepatocellular carcinoma from other hepatic malignancies in patients at risk: diagnostic performance of the liver imaging reporting and data system version 2014. J Radiol 2018;286:158-72.

14. Kim M-J, Lee S, An C. Problematic lesions in cirrhotic liver mimicking hepatocellular carcinoma. Eur J Radiol. 2019;29:5101-10.

15. Kim Y-Y, Kim M-J, Kim EH, Roh YH, An C. Hepatocellular carcinoma versus other hepatic malignancy in cirrhosis: performance of LI-RADS version 2018. J Radiol 2019;291:72-80.

16. Lee HS, Kim M-J, An C. How to utilize LR-M features of the LI-RADS to improve the diagnosis of combined hepatocellular-cholangiocarcinoma on gadoxetate-enhanced MRI? Eur J Radiol. 2019;29:2408-16.

17. Cerny M, Bergeron C, Billiard J-S, Murphy-Lavallée J, Olivié D, Bérubé J, et al. LI-RADS for MR imaging diagnosis of hepatocellular carcinoma: performance of major and ancillary features. J Radiol 2018;288:118-28.

18. Joo I, Lee JM, Lee DH, Ahn SJ, Lee ES, Han JK. Liver imaging reporting and data system v2014 categorization of hepatocellular carcinoma on gadoxetic acid-enhanced MRI: Comparison with multiphasic multidetector computed tomography. J Magn Reson Imaging. 2017;45:731-40.

19. Ronot M, Fouque O, Esvan M, Lebigot J, Aubé C, Vilgrain V. Comparison of the accuracy of AASLD and LI-RADS criteria for the non-

invasive diagnosis of HCC smaller than 3 cm. J Hepatol. 2018;68:715-23.

20. Choi J-Y, Cho HC, Sun M, Kim HC, Sirlin CB. Indeterminate observations (liver imaging reporting and data system category 3) on MRI in the cirrhotic liver: fate and clinical implications. AJR Am J Roentgenol. 2013;201:993-1001.

21. Jeong YY, Mitchell DG, Kamishima T. Small (< 20 mm) enhancing hepatic nodules seen on arterial phase MR imaging of the cirrhotic liver: clinical implications. AJR Am J Roentgenol. 2002;178:1327-34.